2016 13th International Conference on Electrical Engineering, Computing Science and Automatic Control (CCE)
Mexico City. Mexico September 26-30, 2016

UV Electroluminescence from ITO/SRO/p-Si and ITO/SRN/SRO/p-Si Structures

Santiago A. Cabañas-Tay, and Alfredo Morales-Sánchez
Monterrey Unit-PIIT
CIMAV
Apodaca, Nuevo Leon, Mexico
e-mail: scabanastay@hotmail.com, alfredo.morales@cimav.edu.mx.

Liliana Palacios-Huerta, and Mariano Aceves-Mijares
Electronics Department
INAOE
Tonantzintla, Puebla, Mexico
e-mail: lilis.palacios@gmail.com, maceves@ieee.org.

***Abstract*—This work presents the electrical and electroluminescent properties of light emitting capacitors (LECs) using silicon rich oxide (SRO) and the effect of a thin silicon rich nitride (SRN) film on it (SRN/SRO) as active layers. LECs were fabricated using simple Metal–Insulator–Semiconductor (MIS) structures with indium tin oxide (ITO) and aluminum as gate and substrate electrodes, respectively. All devices exhibit a resistance switching (RS) behavior from a high conduction state (HCS) to a low conduction state (LCS), enhancing an intense ultraviolet-blue (UV-B) EL. This RS behavior produces structural changes in the active layer and probably in the ITO contact. Seven narrow bands with half-peak width of 7±0.6 nm at ~250, 270, 285, 305, 325, 415 and 450 nm are clearly observed once the low conduction state is reached. The red-near infrared EL at HCS is similar to the PL spectra indicating the same radiative process is involved. An increment of the EL band at ~590 nm in SRN/SRO is observed at both conduction states. This band has been observed before and attributed transitions from the minimum band conduction to K^0 centers in SRN films. The UV-B emission appears at lower electric field when the SRN/SRO film is used as active layer.**

Keywords—UV electroluminescence, resistive switching, silicon-rich oxide, silicon-rich nitride.

I. INTRODUCTION

Recent research has demonstrated strong visible electroluminescence (EL) from silicon rich oxide (SRO)- or silicon rich nitride (SRN)-based devices as active layer [1-4]. This EL emission has been observed through the shine dots and whole area luminescence [1-4]. Both EL emissions could be together at the same time or appear independently under some conditions. The emission mechanism is different for each one, and their current-voltage characteristic is strongly related to the EL type. Usually, the shine dots emission appear in the high conduction state (HCS) at low voltages, while the whole area emission in the low conduction state (LCS) at high voltages [3, 4]. Structural factors like the presence of amorphous or crystalline silicon nanoparticles (Si-nps) and point defects in the SRO matrix can dramatically affect its optical and electro-optical properties. Besides, structural changes can be produced by the annihilation of preferential conductive paths (created by Si-nps) inside the SRO films with a high current flow, which obviously change their electrical and electro-optical behavior, as repoted before [4, 5]. In order to improve the carrier transport, a Si_3N_4 layer, which is transparent to the visible light and with smaller band gap (~ 5.0 eV) than that of SiO_2 (~9.0 eV), is used to facilitate the carrier injection for optoelectronic applications [6]. Therefore, the flow of charge carriers can be improved increasing the transport ability in the active layers. In fact, Si_3N_4 in MOS capacitors is useful as buffer layer between dielectric layer and the metal increasing the efficiency and lifetime of the device [7]. By other hand, SRN films show a blue-green PL [8, 9]. These SRO and SRN films with controlled and uniform silicon content are easily deposited by Low Pressure Chemical Vapor Deposition (LPCVD) [10, 11].

This study shows an intense ultraviolet-blue (UV-B) EL emission from light emitting capacitors (LECs) using SRO and SRN/SRO films as active layer and ITO as gate contact. According to the electro-optical analysis the intense UV-B emission take place at the low conduction state and it appears at lower electric fields in the SRN/SRO-LECs.

II. EXPERIMENT

SRO and SRN/SRO films were deposited on p-type silicon substrates (100) with resistivity of 5-10 Ω-cm by LPCVD. In this technique, the partial pressure ratio of the reactant gases is used to control the silicon content into the films, $Ro=N_2O/SiH_4$ and $R_N=NH_3/SiH_4$ for SRO and SRN, respectively. Ro = 20 and R_N = 80 values were used for the SRO and SRN films, respectively. The SRO film was deposited for 15 min at 730°C while the SRN was deposited onto the SRO film for 4 min at 760 °C. After deposition, the SRO and SRN/SRO structures were thermally annealed at 1100 °C for 180 minutes in N_2 atmosphere to induce the silicon nanocrystals (Si-NCs) formation. We will call the SRO film as M20 and the SRN/SRO film as B20.

Light emitting capacitors (LECs) were fabricated for electrical and electroluminescence studies. Approximately 300 nm thick, indium tin oxide (ITO) film, was deposited onto the surface of the films by RF sputtering with a power of 50 W. Square shaped patterns with area of 1 mm^2 were defined by a photolithography process step to act as anode gate contact. Finally, ~700 nm thick aluminum (Al) film was evaporated onto the backside of the silicon substrates as cathode contact. A

978-1-5090-3511-3/16/$31.00 ©2016 IEEE

thermal annealing process at 460°C in N_2 atmosphere for 20 min was made to form the ohmic contact.

The thicknesses of thermally annealed SRO and SRN films are 55.2±4.88 and 19.3±1.06 nm, as measured with a Gaertner L117 ellipsometer with a 70° incident laser with wavelength of 632.8 nm. The photoluminescence (PL) and PL excitation (PLE) spectra were measured with a Fluoromax 3 of Horiba Jobin Yvon. The samples were excited using a 300 nm radiation and the PL emission signal was collected from 400 to 900 nm with a resolution of 1 nm. PLE spectra were measured from 200-450 nm with a resolution of 1 nm with the detector centered at the wavelength of maximum PL emission for each film. The composition in depth profile of thermally annealed SRO and SRN/SRO films was analyzed by means of X-ray photoelectron spectroscopy (XPS) Escalab 250Xi of Thermo Scientific equipment, with an Al Kα monochromated source. Current-voltage (I-V) measurements of SRO and SRN/SRO-LECs were performed using a Keithley 4200-SCS parameter analyzer at the same time that the EL was collected with an optical fiber, which was located right on the surface of the device and connected to an Ocean Optics QE-65000 spectrometer. For the electrical characterization, the substrate was grounded and the ITO was negative for the forward bias.

III. Results and Discussion

Figure 1 a) shows the composition in depth profile of the thermally annealed SRO monolayer and SRN/SRO bilayer, both with Ro=20 (M20 and B20, respectively). The average Si content within the SRO monolayer was about 41.85±1.1 at.%. When the SRN/SRO bilayer is formed, the oxide-nitride interface becomes an imprecise oxynitride (SiON) layer (shadow area). In that region, a gradual increasing of both nitrogen and silicon was observed towards the interface. The average Si content slightly increases up to ~43.21±0.7 at.% in the SRO layer. While, the oxygen content in the SRO film reduces from 56.78±1.3 to 53.08±1.0 at.%. The Si, O and N diffusion could be enhanced by the high annealing temperature. This is supported by two facts: first, the presence of a nitrogen concentration within the oxide layer which goes from 2 to 10 %, and second, the oxygen presence in the nitride layer (~25%).

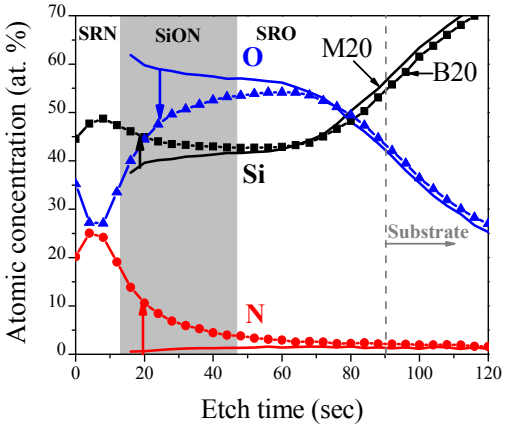

Fig. 1. Depth profile of atomic concentration of Si, O, N of SRO (M20) and SRN/SRO (B20) films after thermal annealing.

The nitrogen content inside of the SRO layer in the SRN/SRO bilayer structure could modify its optical and structural properties. It has been reported that the nitrogen hinder the diffusion of Si atoms and prevents the phase separation in the amorphous SiOx:N films [12]. Thus, the mobility of the Si atoms is slower and the growth of the Si-nps during the thermal diffusion process is reduced, giving as result smaller Si-nps.

The normalized photoluminescence (PL) spectra of SRO and SRN/SRO samples annealed at 1100°C are shown in Fig 2. The SRO film (M20) emits a visible-red-luminescence and an additional band placed at ~420 nm due to the presence of weak oxygen bonds (WOB) [13, 14]. It has been reported that this additional band is more intense in SRO samples with high silicon excess (>5%) [14]. In spite of the efforts that the scientific community has made to understand the origin of the luminescent emission in SRO films, the mechanism of light emission has not yet completely understood. Defects, Si-nps, as well as interaction between defects at the SiO_2/Si interface have been proposed as the origin of luminescence in SRO. The presence of Si-nps in SRO films has been using an Energy Filtered Transmission electron Microscopy (EFTEM) in previous work [15]. It was found that the average Si-nps size changes according to the silicon excess, being 2.7 nm for SRO with ~5.1 at.% and 4.1 nm with ~12.7 at.%. Therefore, the red luminescence from SRO films after thermal annealing results of the presence of Si-nps [14]. On the other hand, it is possible to observe that the PL spectrum becomes narrow and it slightly blue-shifts when a SRN film is placed on top of the SRO film. A blue-shift is expected when the size of Si-nps is reduced according with the quantum confinement effect (QCE) [16-19]. Therfore, the observed blue-shift is probably due to a reduction of the Si-nps size increasing the violet-yellow band in the SRN/SRO film.

To understand the PL emission, room temperature photoluminescence excitation (PLE) measurements were made. PLE spectra were measured for the maximum PL band. A broad PLE spectra from ~230 nm to ~450 nm composed by two apparent bands at ~295 nm and ~365 nm are observed. Although these two bands have been related with the presence of amorphous and crystalline Si-nps [20], the broad PLE spectra include absorption wavelengths of some defects.

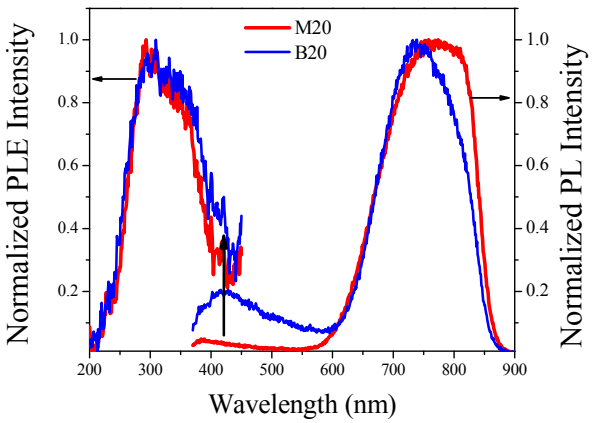

Fig. 2. Normalized PL and PLE spectra of thermally annealed SRO (M20) and SRN/SRO (B20) films.

In fact, a shoulder at ~420 nm is observed in the PLE spectra for both SRO and SRN/SRO films and its intensity increases when the SRN/SRO films is formed. This absorbance band at ~420 nm coincides with a PL band at 420 nm. An increase in the 420 nm PLE band results in an increased 420 nm PL band in the SRN/SRO film. Therefore, this band could be related to electronic transitions from K^0 centers to the maximum of valence band (MBV) into SRN films, as reported before [11].

In order to know the electro-optical properties in the SRO and SRN/SRO based LECs, current density-electric field (J-E) characteristic were measured, as shown in figure 3. The electric field, given by the voltage divided by the active layer thickness, has been increased as much as possible before dielectric breakdown. Figure 3 a) shows the J-E characteristic of the SRO-LEC. In this device, a current density drop from a high conduction state (HCS, ~5 Acm^{-2}) to a low conduction state (LCS, ~ 8×10^{-3} Acm^{-2}) is observed when the electric field reaches ~2.5 $MVcm^{-1}$. Recent studies regarding to the resistive switching behavior in SRO films was observed before and related with a conductive filament, showing that the conductance drop is related with a crystallization and an amorphization process of Si-nps that creates the conductive filament, besides the creation of point defects [21-23]. After that, the current rises abruptly from LCS (~3×10^{-3} Acm^{-2}) to HCS (~8 Acm^{-2}) when the electric field reaches ~3.75 $MVcm^{-1}$.

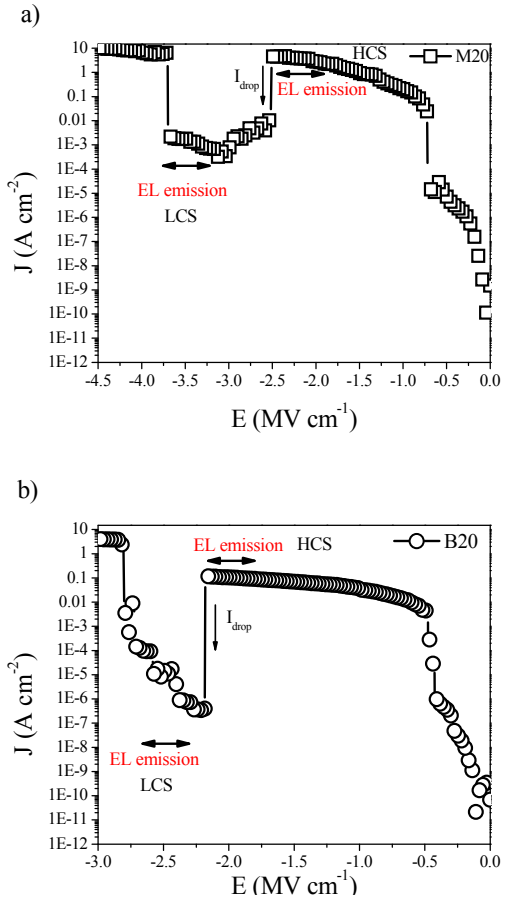

Fig. 3. J-E characteristic of a) SRO-LEC, and b) SRN/SRO-LEC.

It has been reported when a high electric field is applied (~1 $MVcm^{-1}$) between the electrodes, a severe decomposition of ITO takes place. Thus, the ions of indium or tin might migrate into the active layer due the joule heating contributing of the creation the electrical paths between the two electrodes increasing the current [24]. However, when the SRN/SRO film is formed the current density drop appears at lower electric fields (~2$MVcm^{-1}$), as shown in figure 3 b). Moreover, the current rises more slowly from LCS to HCS at ~2.75 $MVcm^{-1}$. This injection current enhancement is obviously due to the incorporation of the SRN layer. If we compare the current densities of both LECs, the values found in the SRN/SRO-based LEC are lower than that SRO-based LEC. This could suggest that the SRN/SRO bilayer contains fewer matrix defects or smaller Si-nps, leading to a lower conductivity.

Figure 4 a) shows EL spectra and images of the SRN/SRO-based LEC (B20) obtained at HCS when the applied forward bias is -17V, -18V and -19V, respectively. The EL spectrum is broad and their position does not change when the voltage increases. The emission is observed with the naked eye as shine dots on the surface of the device, as shown in the images. A similar emission through shine dots is also observed in the SRO-LEC (M20) (not shown here). Figure 4 b) shows EL spectra and images of the same device obtained after the LCS is reached and for different forward bias voltajes. The EL emission is observed in two wavelength regions: first, seven sharp emission lines appeared in the spectral range from ultraviolet to blue (UV-B) at ~250, ~270, ~285, ~305, ~325, ~415 and ~450 nm with half-peak width of all the lines as low as 7±0.6 nm. The intensity of these sharp EL lines increases but keep their position when the voltage increases. The second emission is observed in the red and near infrared region (R-NIR) a broad EL band of low intensity with the maximum emission at ~750 nm. The emission also keeps their shape and growths when the voltage increases. As it can be seen in the images, the emission are violet-blue shine dots randomized on the surface contact. When the current increases they increase their intensity and more dots appear. A similar emission through shine violet-blue dots is also observed in the LEC M20 (not shown here). The UV EL spectrum of M20-based LEC also shows the same seven peaks at the same position as shown in the inset of figure 4 b).

Four narrow emission bands with half-peak width of 4 nm at 293.78 nm, 316.10 nm, 403.07 nm, and 444.82 nm were reported by X. Yin et. al. from ITO/Y_2O_3/Ag structures [25]. These emission bands were attributed to the characteristic radiation of Indium ions. The most intense emission bands of our samples are very similar to those observed by X. Yin et. al. but displaced ~10 nm to longer wavelengths. Thereby, these narrow bands could have a similar origin. However, the less intense bands were not observed by X. Yin et. al., so a further study should be done.

The light emission mechanism in silicon based materials has not been understood completely. Depending on the wavelength, multiple luminescent centers such as defects, Si-nps, as well as the interaction of defects on the Si-nps/SiO_2 interface have been reported.

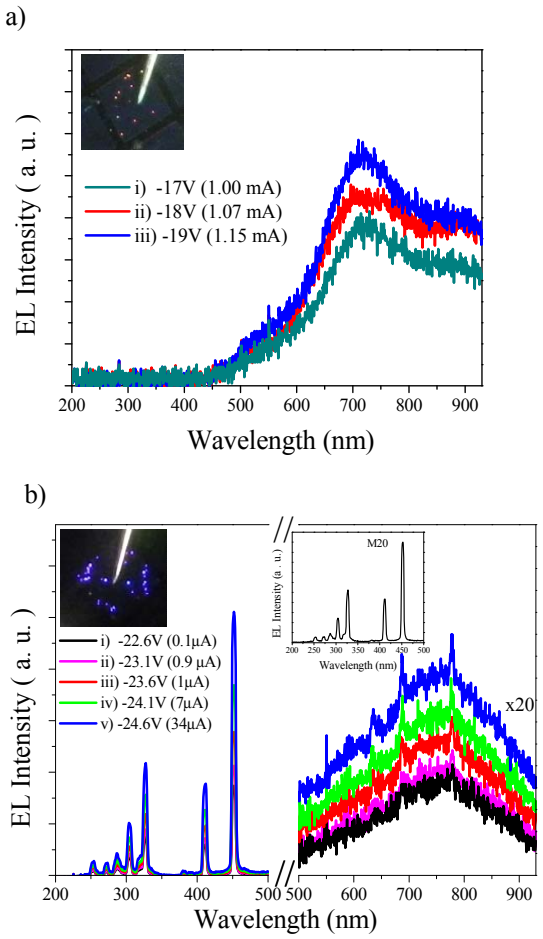

Fig. 4. EL spectra of the SRN/SRO-LEC for different injected currents at a) high conduction state (HCS), and b) low conduction state (LCS). At the top, picture of the device at the higher injected current for each conduction state. The inset shows the UV EL for the SRO-LEC (M20) at LCS.

The EL and PL spectra of SRO (M20) and SRN/SRO (B20) films at low voltages range (when HCS is obtained) have been compared in figure 5.

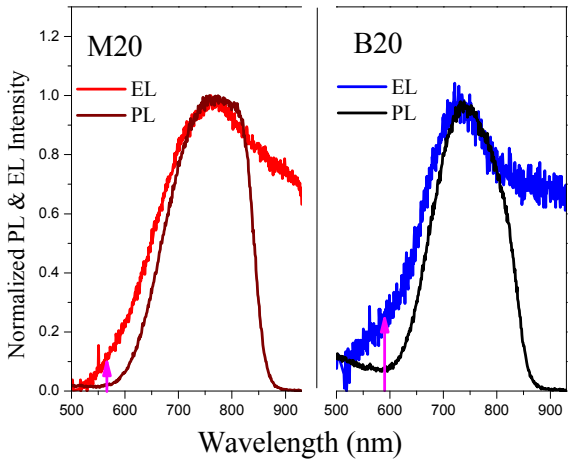

Fig. 5. Correlation between PL and EL spectra of SRO film (left side) and SRN/SRO film (right side). The EL emission is taken in the high conduction state (HCS).

The central emission wavelength of EL and PL for both samples is not deviated from each other; this overlap indicates that the origin of the light emission is the same. However, the broad EL spectrum show the presence of some defects such as E'ẟ defect (emission at 560 nm) and K^0 centers (emission at 590 nm, only in B20), which are also pumped under high biases [26, 27]. Moreover, the intensity of EL emission bands at 560 nm and 590 nm increases after the electro-forming, so that it could be related to the creation of a greater number of defects.

IV. Conclusion

The composition, luminescent and electrical properties of SRO and SRN/SRO films deposited by LPCVD were studied. When the SRN is deposited on the SRO to form the bilayer some compositional changes are observed. A resistive switching from a HCS to a LCS is observed in both SRO and SRN/SRO based LECs. A red EL at HCS is observed and similar to the PL spectra indicating the same radiative process is involved for both samples. An enhancement of the EL band at ~590 nm in SRN/SRO is observed at both high and low conduction states. This band has been observed before and attributed to transitions from the minimum conduction band to K^0 centers in SRN films. An intense UV-B EL at high electric fields and LCS is also observed for both samples, and it is related to indium ions radiation.

Acknowledgment

S. A. Cabañas-Tay and L. Palacios-Huerta acknowledge the support received from CONACYT through the grants 319852 and 226227, respectively. This work has been partially supported by the project CONACyT-180992. Authors want to thank technicians Pablo Alarcon and Luis Gerardo Silva from INAOE and CIMAV, respectively.

References

[1] G.-R. Lin, C.-H. Chang, C.-H. Cheng, C.-I. Wu, and P.-S. Wang, "Transient UV and Visible Luminescent Dynamics of Si-Rich SiOx Metal-Oxide-Semiconductor Light-Emitting Diodes", *IEEE Photonics J.* **4**(5), 1351-1364 (2012); DOI: 10.1109/JPHOT.2012.2209633

[2] M. Xie, D. Li, F. Wang, and D. Yang, "Luminescence Properties of Silicon-Rich Silicon Nitride Films and Light Emitting Devices", *ECS Transactions*, **35** (18), 3-19 (2011); DOI: 10.1149/1.3647900.

[3] A. Morales-Sanchez, K. Monfil-Leyva, A. A. González, M. Aceves-Mijares, J. Carrillo, J. A. Luna-López, C. Domínguez, J. Barreto, and F. J. Flores-Gracia, "Strong blue and red luminescence in silicon nanoparticles based light emitting capacitors", *Appl. Phys. Lett.* **99**, 171102 (2011); DOI: 10.1063/1.3655997.

[4] A. Morales-Sanchez, J. Barreto, C. Domínguez, M. Aceves-Mijares, M. Perálvarez, B. Garrido, and J. A. Luna-López, "DC and AC electroluminescence in silicon nanoparticles embedded in silicon-rich oxide films", *Nanotechnology* **21**(8), 085710 (2010); DOI: 10.1088/0957-4484/21/8/085710.

[5] A Morales-Sánchez, J Barreto, C Domínguez, M Acevesand J A Luna-López, "The mechanism of electrical annihilation of conductive paths and charge trapping in silicon-rich oxides", *Nanotechnology* **20**(4), 045201 (2009); DOI: 10.1088/0957-4484/20/4/045201.

[6] X. Wang, R. Huang, C. Song, Y. Guo, and J. Song, "Effect of barrier layers on electroluminescence from Si/SiOxNy multilayer", *Appl. Phys. Lett.* **102**(8), 081114, (2013); DOI: 10.1063/1.4794079.

[7] M. Perálvarez, J. Carreras, J. Barreto, A. Morales, C. Domínguez, and B. Garrido, "Efficiency and reliability enhancement of silicon nanocrystal field-effect luminescence from nitride-oxide gate stacks", *Appl. Phys. Lett*. **92**(24), 241104 (2009); DOI: 10.1063/1.2939562.

[8] M.-S. Yang, K.-S. Cho, J.-H. Jhe, S.-Y. Seo, J. H. Shin, K. J. Kim, and D. W. Moon, "Effect of nitride passivation on the visible photoluminescence from Si-nanocrystals", *Appl. Phys. Lett.* **85**(16), 3408-3410 (2004); DOI: 10.1063/1.1787599.

[9] A.A. González, M. Aceves-Mijares, A. Morales-Sánchez, and K. Monfil-Leyva, "Intense whole area electroluminescence from low pressure chemical vapor deposition-silicon-rich oxide based light emitting capacitors", *J of Appl Phys.* **108**(4), 043105 (2010); DOI: 10.1063/1.3465335.

[10] A. Morales, J. Barreto, C. Domínguez, M. Riera, M. Aceves, and J. Carrillo, "Comparative study between silicon-rich oxide films obtained by LPCVD and PECVD", *Physica E* **38**(1-2), 54-58 (2007); DOI: 10.1016/j.physe.2006.12.056

[11] S. A. Cabañas-Tay, L. Palacios-Huerta, J. A. Luna-López, M. Aceves-Mijares, S. Alcántara-Iniesta, S. A. Pérez-García, and A. Morales-Sánchez, "Analysis of the luminescent centers in silicon rich silicon nitride light-emitting capacitors", *Semicond. Sci. Technol*. **30**(6), 065009 (2015); DOI: 10.1088/0268-1242/30/6/065009.

[12] B. H. Augustine, E. A. Irene, Y. J. He, K. J. Price, L. E. McNeil, K. N. Christensen, and D. M. Maher, "Visible light emission from thin films containing Si, O, N, and H", *J. Appl. Phys.* **78**(6), 4020-4030 (1995); DOI: 10.1063/1.359925

[13] F. Flores Gracia, M. Aceves, J. Carrillo, C. Domínguez, and C. Falcony, "Photoluminescence and cathodoluminescence characteristics of SiO_2 and SRO films implanted with Si", *Superficies y Vacío* **18**(2) 7-13 (2005); http://www.fis.cinvestav.mx/~smcsyv/supyvac/18_2/SV1820705.pdf

[14] A. Morales-Sánchez, K.M. Leyva, M. Aceves, J. Barreto, C. Domínguez, J.A. Luna-López, J. Carrillo, J. Pedraza, "Photoluminescence enhancement through silicon implantation on SRO-LPCVD films", *Materials Science and Engineering B* **174**, 119-122 (2010); DOI: 10.1016/j.mseb.2010.03.031.

[15] A. Morales-Sánchez, J. Barreto, C. Domínguez-Horna, M. Aceves-Mijares, and J. A. Luna-López, "Optical characterization of silicon rich oxide films", *Sensors and Actuactors A* **142**(1),12-18 (2008); DOI: 10.1016/j.sna.2007.03.008.

[16] N. M. Park, T. S. Kim, and S. J. Park, "Band gap engineering of amorphous silicon quantum dots for light-emitting diodes", *Appl. Phys. Lett.* **78**(17), 2575 (2001); DOI:10.1063/1.1367277.

[17] T. Y. Kim, N. M. Park, K. H. Kim, G. Y. Sung, Y. W. Ok, T. Y. Seong, and C. J. Choi, "Quantum confinement effect of silicon nanocrystals in situ grown in silicon nitride films", *Appl. Phys. Lett.* **85**(22), 5355 (2004); DOI: 10.1063/1.1814429.

[18] C. Delerue, G. Allan, and M. Lannoo, "Theoretical aspects of the luminescence of porous silicon", *Phys. Rev. B*. **48**(15), 11024-11036 (1993); DOI: 10.1103/PhysRevB.48.11024.

[19] C. L. Wu, and G.-R. Lin, "Power Gain Modeling of Si Quantum Dots Embedded in a SiO bmx Waveguide Amplifier With Inhomogeneous Broadened Spontaneous Emission", *IEEE J. Sel. Topics Quantum. Electron.* **19**(5), 3000109 (2012); DOI: 10.1109/JSTQE.2012.2222357

[20] A. Podhorodecki, G. Zatryb, L. W. Golacki, J. Misiewicz, J. Wojcik, and P. Mascher, "On the origin of emission and thermal quenching of SRSO:Er^{3+} films grown by ECR-PECVD", *Nanoscale Research Letters* **8**, 98 (2013); DOI: 10.1186/1556-276X-8-98.

[21] J. Yao, Z. Sun, L. Zhong, D. Natelson and J. M. Tour, "Resistive Switches and Memories from Silicon Oxide", *Nano Letters* **10**(10), 4105-4110 (2010); DOI: 10.1021/nl102255r.

[22] J. Yao, L. Zhong, D. Natelson, and J. M. Tour, "In situ imaging of the conducting filament in a silicon oxide resistive switch", *Scientific Reports* **2**, 242 (2012); DOI: 10.1038/srep00242.

[23] A.Mehonic, A.Vrajitoarea, S.Cueff, S.Hudziak, H. Howe, C. Labbé, R.Rizk, M. Pepper, and A. J. Kenyon, "Quantum Conductance in Silicon Oxide Resistive Memory Devices", *Scientific Reports* **3**, 2708 (2013); DOI: 10.1038/srep02708.

[24] J. He, M. Lu, X. Zhou, J. R. Cao, K. L. Wang, L. S. Liao, Z. B. Deng, X. M. Ding, X. Y. Hou, and S. T. Lee, "Damage study of ITO under high electric field", *Thin Solid Films* **363**(1-2), 240-243 (2000); DOI: 10.1016/S0040-6090(99)01066-4.

[25] X. Yin, S. Wang, L. Li, G. Mu, Y. Tang, W. Duan, and L. Yi, "Intense deep-blue electroluminescence from ITO/Y_2O_3/Ag structure", *Optics Express* **23**(14), 018092 (2015); DOI: 10.1364/OE.23.018092.

[26] Z. Pei, Y. R. Chang, and H. L. Hwang, "White electroluminescence from hydrogenated amorphous-SiNx thin films", *Appl. Phys. Lett*. **80**(16), 2839 (2002); DOI: 10.1063/1.1473230.

[27] S.-T. Chou, J.-H. Tsai, and B.-C. Sheu, "The photoluminescence in Si^+-implanted SiO_2 films with rapid thermal anneal", *Journal of Applied Physics* **83**(10), 5394-5398 (1998); DOI: 10.1063/1.367368.